SIMPLE COOPERATIVE TRANSMISSION SCHEMES FOR UNDERLAY SPECTRUM SHARING USING SYMBOL-LEVEL PRECODING AND LOAD-CONTROLLED ARRAYS

K. Ntougias, D. Ntaikos, C. B. Papadias

Athens Information Technology
B-WiSE
Athens, Greece
E-mail: {kontou, dint, cpap}@ait.gr

*G. K. Papageorgiou**

Heriot-Watt University
ISSS of EPS
Edinburgh, UK
E-mail: g.papageorgiou@hw.ac.uk

ABSTRACT

The combination of coordinated multi-point (CoMP) and underlay spectrum sharing promises substantial spectral efficiency (SE) gains for future cellular networks. However, this concept has been largely overlooked in the literature. Moreover, none of the few relevant studies consider the use of "standard" transmission strategies to facilitate the adoption of the aforementioned communication paradigm by 5G networks.

The use of load-controlled antenna arrays (LC-AA) and symbol-level (SL) precoding can further enhance the performance of CoMP cellular networks, as it has been shown in the literature. Nevertheless, the corresponding research works do not consider a spectrum sharing setup.

In this paper, we fill this gap in the literature by deriving the optimal power allocation strategy (in the sum-SE sense) and the corresponding algorithm that implements this solution for scenarios where various linear or SL precoding schemes are applied. Numerical simulations indicate the feasibility of the proposed approach for LC-AA-equipped CoMP networks and shed light on the effect of various parameters on system performance.

***Index Terms*—** Coordinated multi-point (CoMP), non-orthogonal spectrum sharing (NOSS), load-controlled antenna arrays (LC-AA), joint beam selection and precoding algorithm (JBSPA), symbol-level zero-forcing beamforming (SL-ZFBF).

1. INTRODUCTION

Sub-6 GHz spectrum will be an important part of the 5G landscape [1]. The scarcity of resources in this spectral region [2] and the stringent capacity requirements of the envisioned services [3], though, necessitate the use of technologies that increase the spectral efficiency (SE), such as spectrum sharing [4–6] and coordinated multi-point (CoMP) [7].

Among the various "flavors" of the former communication paradigm, the so-called underlay spectrum sharing provides the greater SE gains [6]. CoMP can further increase the sum-SE of cellular networks in such non-orthogonal spectrum sharing (NOSS) setups, in comparison to legacy uncoordinated communication methods, due to its advanced resource allocation and interference management features [7]. Surprisingly enough, though, the literature includes only a handful of works that consider the NOSS problem from the aforementioned 5G perspective [7, 8]. These studies derive the optimal precoders for relaxed versions of the original non-convex optimization problem. Nevertheless, none of them consider the application of "standard" linear precoding schemes, which would relax the sum-SE maximization problem into an optimal power allocation task and could accelerate the adoption of NOSS by future cellular networks.

Load-controlled antenna arrays (LC-AA) can further enhance the performance of cellular networks, thanks to their high array gain [9]. On the other hand, performing arbitrary precoding with LC-AAs is a challenging task due to limitations regarding the loading values [10, 11]. A joint beam selection and precoding algorithm (JBSPA) that utilizes analog beamforming and digital precoding as a simple workaround to this problem in CoMP setups is presented in [12–15]. In [13] the authors study also the application of symbol-level (SL) zero-forcing beamforming (ZFBF) in such setups, which improves the performance in the low signal-to-noise-ratio (SNR) regime by exploiting the constructive SL-interference. However, these works do not consider spectrum sharing.

In this paper, we aspire to fill this gap in the literature. To this end, we consider the application of ZFBF in a spectrum sharing agnostic manner to relax the sum-SE maximization problem to a convex optimization task [7]. Then, we derive the optimal coordinated power allocation scheme for these precoders and present its implementation algorithm. The performance of the proposed NOSS strategy is evaluated via numerical simulations for LC-AA-equipped setups that make use of several beam selection and linear precoding schemes—both codeword-level and symbol-level.

*G. K. Papageorgiou performed the work while at Athens Information Technology.

2. SYSTEM SETUP AND ASSUMPTIONS

A NOSS setup is considered in this paper. The secondary system (SS) consists of M base stations (BS), where each one has N antennas and serves K active single-antenna mobile stations (MS). The primary system (PS), on the other hand, is comprised by a single-input single-output (SISO) link. The m-th BS and the k-th MS in the m-th cell are denoted as BS_m and MS_{km}, whereas the transmitter and the receiver of the PS are denoted as $\mathrm{TX}_{\mathrm{PS}}$ and $\mathrm{RX}_{\mathrm{PS}}$, respectively (see Fig. 1).

The following assumptions are in order: (i) Quasi-static frequency-flat Rayleigh fading channels are considered. (ii) The SS adopts universal frequency re-use. (iii) The whole SS is considered as a single cooperation cluster. This assumption facilitates the study of the proposed techniques behavior. (iv) The coordination decisions are taken by a master BS [7, 16–18]. (v) The coordinated beamforming (CBF) cooperation variant is utilized, where the cooperating BSs serve disjoint groups of users [7, 16–18]. (vi) All nodes make use of perfect channel state information (CSI).

3. SIGNAL AND CHANNEL MODELS

The complex baseband representation of the received signal at MS_{km}, $y_{km} \in \mathbb{C}$, is given by:

$$\begin{aligned} y_{km} = {} & \left(\mathbf{h}_{km}^{m}\right)^{\dagger} \mathbf{w}_{mk}^{m} \sqrt{P_{mk}^{m}} s_{mk}^{m} \\ & + \sum_{\substack{i=1 \\ i \neq k}}^{K} \left(\mathbf{h}_{km}^{m}\right)^{\dagger} \mathbf{w}_{mi}^{m} \sqrt{P_{mi}^{m}} s_{mi}^{m} \\ & + \sum_{\substack{j=1 \\ j \neq m}}^{M} \sum_{l=1}^{K} \left(\mathbf{h}_{km}^{j}\right)^{\dagger} \mathbf{w}_{jl}^{l} \sqrt{P_{jl}^{j}} s_{li}^{j} \\ & + h_{km} \sqrt{P} d + n_{km}, \end{aligned} \tag{1}$$

for $k = 1, \ldots, K$ and $m = 1, \ldots, M$. In Eq. (1) and all subsequent equations, the time index is omitted, for convenience. The terms in the right-hand side (RHS) of Eq. (1) are, in order, the data signal, the intra-cell co-channel interference (CCI), the inter-cell CCI, the inter-system CCI caused by the transmission of the PS, and the additive white Gaussian noise (AWGN) at MS_{km}. More specifically, $\mathbf{h}_{km}^{m} \sim \mathcal{CN}\left(\mathbf{0}_N, \left(\sigma_{km}^{m}\right)^2 \mathbf{I}_N\right)$ is the channel between MS_{km} and BS_m; $\mathbf{w}_{mk}^{m} \in \mathbb{C}^N$ is the BF vector of BS_m that is associated with MS_{km}; $P_{mk}^{m} \in \mathbb{R}_+$ is the transmission power that is allocated to MS_{km} by BS_m; $s_{mk}^{m} \in \mathbb{C}$ is the symbol that is transmitted from BS_m to MS_{km}; $h_{km} \in \mathcal{CN}\left(0, \left(\sigma_{km}\right)^2\right)$ is the channel between MS_{km} and $\mathrm{TX}_{\mathrm{PS}}$; $P \in \mathbb{R}_+$ is the transmission power of $\mathrm{TX}_{\mathrm{PS}}$; $d \in \mathbb{C}$ is the symbol that is transmitted by $\mathrm{TX}_{\mathrm{PS}}$ to $\mathrm{RX}_{\mathrm{PS}}$; and $n_{km} \sim \mathcal{CN}(0,1)$ is the AWGN at MS_{km}. Note that $\|\mathbf{w}_{mk}^{m}\| = 1$ and $\mathbb{E}\left[\left|s_{mk}^{m}\right|^2\right] = \mathbb{E}\left[|d|^2\right] = 1$.

The complex baseband representation of the received signal at $\mathrm{RX}_{\mathrm{PS}}$, $y \in \mathbb{C}$, is given by:

$$y = g\sqrt{P} d + \sum_{m=1}^{M} \sum_{k=1}^{K} \mathbf{g}_m^{\dagger} \mathbf{w}_{mk}^{m} \sqrt{P_{mk}^{m}} s_{mk}^{m} + z. \tag{2}$$

The terms in the RHS of Eq. (2) are, in order, the data signal; the inter-system CCI at $\mathrm{RX}_{\mathrm{PS}}$ that is caused by the transmissions of the M BSs; and the AWGN at $\mathrm{RX}_{\mathrm{PS}}$. More specifically, $g \sim \mathcal{CN}\left(0, \sigma^2\right)$ is the channel between $\mathrm{RX}_{\mathrm{PS}}$ and $\mathrm{TX}_{\mathrm{PS}}$; $\mathbf{g}_m \sim \mathcal{CN}\left(\mathbf{0}_N, \left(\sigma_m\right)^2 \mathbf{I}_N\right)$ is the channel between $\mathrm{RX}_{\mathrm{PS}}$ and BS_m; and $z \sim \mathcal{CN}(0,1)$ is the AWGN at $\mathrm{RX}_{\mathrm{PS}}$.

Eq. (1) can be expressed in matrix form as:

$$\mathbf{y} = \mathbf{H}_{SS} \mathbf{W} \mathbf{P}^{1/2} \mathbf{s} + \sqrt{P} \mathbf{h} d + \mathbf{n}, \tag{3}$$

where $\mathbf{y} \in \mathbb{C}^{K_T}$ is the vector of received symbols at the $K_T = MK$ MSs; $\mathbf{H}_{SS} \in \mathbb{C}^{K_T \times N_T}$ is the composite channel between the K_T single-antenna MSs and the $N_T = MN$ antennas of the M BSs; $\mathbf{W} \in \mathbb{C}^{N_T \times K_T}$ is the precoding matrix; $\mathbf{P} \in \mathbb{R}^{K_T \times M}$ is the power allocation matrix; $\mathbf{s} \in \mathbb{C}^M$ is the vector of transmitted symbols; $\mathbf{h} \in \mathbb{C}^{K_T}$ is the channel that is formed between the $\mathrm{TX}_{\mathrm{PS}}$ and the K_T MSs; and $\mathbf{n} \in \mathbb{C}^{K_T}$ is the noise vector. We consider the application of ZFBF in a spectrum sharing agnostic manner to diagonalize the composite channel (i.e., $\mathbf{W}^{(\mathrm{ZF})} = \left(\mathbf{H}_{SS}\right)^{+}$) and, thus, eliminate the intra-SS CCI [19]. Then, the signal-to-interference-plus-noise-ratio (SINR) at MS_{km} is [12]:

$$\gamma_{km} = \frac{\left|\left(\mathbf{h}_{km}^{m}\right)^{\dagger} \left(\mathbf{w}_{mk}^{m}\right)^{(\mathrm{ZF})}\right|^2 P_{mk}^{m}}{\left|h_{km}\right|^2 P + 1}. \tag{4}$$

4. PROBLEM FORMULATION AND SOLUTION

After the application of ZFBF, the sum-SE maximization problem reformulates into a convex power allocation task:

$$\min_{P_{mk}^{m}} \quad -R = -\sum_{m=1}^{M} \sum_{k=1}^{K} \log_2\left(1 + \gamma_{km}\right) \tag{5a}$$

s.t.

$$P_{mk}^{m} \geq 0, \quad k = 1, \ldots, K;\ m = 1, \ldots, M \tag{5b}$$

$$\sum_{k=1}^{K} P_{mk}^{m} \leq P_T, \quad m = 1, \ldots, M \tag{5c}$$

$$\sum_{m=1}^{M} \sum_{k=1}^{K} \left|\mathbf{g}_m^{\dagger} \left(\mathbf{w}_{mk}^{m}\right)^{(\mathrm{ZF})}\right|^2 P_{mk}^{m} \leq P_I. \tag{5d}$$

Eq. (5a) shows the objective function R, where γ_{km} is given by Eq. (4). Eq. (5b) represents the implicit constraint of non-negative transmission power. Eq. (5c) corresponds to the sum transmission power constraints (SPC), where P_T is the maximum allowed sum-power of each BS. Finally, Eq. (5d) represents the interference power constraint (IPC), where P_I is the interference power threshold (IPT) of $\mathrm{RX}_{\mathrm{PS}}$.

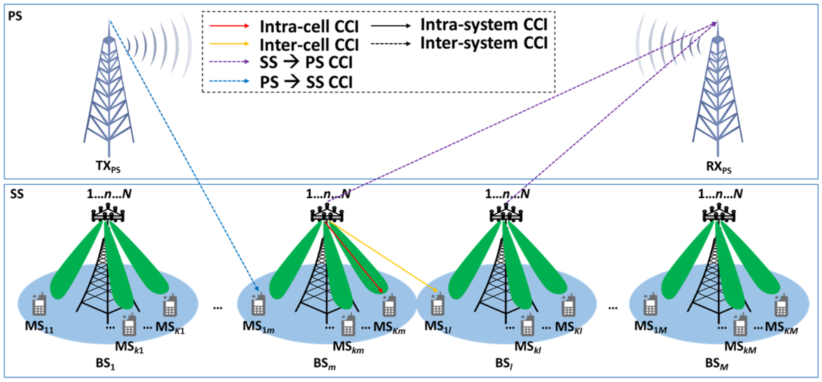

Fig. 1: System setup and types of co-channel interference.

Theorem 1 *By setting:*

$$\lambda_{mk}^{m} = \frac{\left|\left(\mathbf{h}_{km}^{m}\right)^{\dagger}\left(\mathbf{w}_{mk}^{m}\right)^{(ZF)}\right|^{2}}{\left|h_{km}\right|^{2} P + 1}, \tag{6a}$$

$$\alpha_{mk}^{m} = \left|\mathbf{g}_{m}^{\dagger}\left(\mathbf{w}_{mk}^{m}\right)^{(ZF)}\right|^{2}, \tag{6b}$$

the solution to the optimization problem in Eq. (5) is given by the interference-constrained power allocation (ICPA) scheme:

$$P_{mk}^{m} = \left(\frac{1}{\ln 2\left(\nu_m + \mu a_{mk}^{m}\right)} - \frac{1}{\lambda_{mk}^{m}}\right)^{+}, \tag{7}$$

for $m = 1, \ldots, M$ and $k = 1, \ldots, K$, where ν_m and μ are Langrange multipliers.

The proof of Theorem 1 is obtained by taking the Langrangian form of the optimization problem in Eq. (5) and applying the Karush-Kuhn-Tucker (KKT) conditions. It should be noted that this multi-level water-filling (WF) solution can be viewed as a generalization of the one derived in [20] for a single-user multiple-input multiple-output (SU-MIMO) SS instead of a CoMP setup. We should also notice that the derived solution can be applied heuristically to other linear precoding schemes or even to SL ones as well (i.e., as if ZFBF were used [7]). In addition, we should mention that in the high-SNR regime this power allocation strategy is expected to be optimal for the scenario where regularized ZFBF is applied [7, 19].

5. ALGORITHM

The iterative algorithm that implements the solution of Theorem 1 is presented in Algorithm 1. This algorithm calculates the Langrange multipliers ν_m ($m = 1, \ldots, M$) and μ which are related with the SPCs per BS and the IPC, respectively. The algorithm chooses an initial value of μ between a minimum and a maximum value, calculates the minimum values of ν_m for this value such that the SPCs are met, computes the power levels for the given values of the Langrange multipliers according to Eq. (7), and then makes use of the bisection method to update the value of μ based on whether the IPC is met or not. The parameter δ_μ is a positive constant that controls the accuracy of the algorithm. Note that when the IPC is inactive, $\mu = 0$ and the algorithm reduces to the corresponding interference-unconstrained solution, which is used as a benchmark in the performance evaluation section.

Algorithm 1 ICPA Algorithm

```
procedure ICPA(λ^m_mk, α^m_mk, P_T, P_I)
    Initialize: μ_min, μ_max
    while |μ_max − μ_min| > δ_μ do
        μ = (μ_min + μ_max)/2
        for m = 1 to M do
            Find min(ν_m), ν_m ≥ 0 :
            Σ_{k=1}^{K} (P^m_mk)^+ ≤ P_T
        Compute P^m_mk according to Eq. (7)
        if Σ_{m=1}^{M} Σ_{k=1}^{K} a^m_mk P^m_mk ≥ P_I then
            μ_min = μ
        else
            μ_max = μ
    Output: P^m_mk,   m = 1,...,M; k = 1,...,K
```

6. ARBITRARY PRECODING WITH LOAD-CONTROLLED ARRAYS

In Fig. 1 each BS is equipped with a single-fed LC-AA that generates at each given time one out of B possible beams corresponding to B precomputed sets of loading values and serves a single-antenna MS. The system utilizes the JBSPA, which is described as follows [12–15]:

1. **Learning phase:** For each one of the B^M possible M-tuples of beams, the MSs report their SINR or the channel estimates.

2. **Beam selection phase:** The BSs select the optimum M-tuple of beams, in terms of the achieved sum-SE.
3. **Transmission phase:** The BSs transmit digitally precoded signals over the selected beams.

7. SYMBOL-LEVEL ZFBF

The precoding matrix of SL-ZFBF $\mathbf{W}^{(\text{SL-ZF})} \in \mathbb{C}^{N_T \times K_T}$ has the following form [13,21]:

$$\mathbf{W}^{(\text{SL-ZF})} = \mathbf{W}^{(\text{ZF})}\mathbf{T}, \tag{8}$$

where $\mathbf{W}^{(\text{ZF})} \in \mathbb{C}^{N_T \times K_T}$ is the precoding matrix of ZFBF and $\mathbf{T} \in \mathbb{C}^{K_T \times K_T}$ is a modulation-specific matrix that is computed on a symbol-by-symbol basis.

8. PERFORMANCE EVALUATION

We are interested in the average sum-SE per cell over an average receive SNR range of 0 - 30 dB. We assume that the SS is comprised by $M = 2$ BSs equipped with a single-fed LC-AA each that generates at each timeslot one out of $B = 4$ possible beams and serves a single-antenna MS. In the following tests, $P = 0$ dB.

In Fig. 2a the performance of several JBSPA variants for $P_I = 30$ dB is illustrated. We consider also a scenario where the BSs are equipped with a single-fed directive antenna that generates a fixed radiation pattern and utilize ZFBF. We note that the LC-AA-equipped setup outperforms significantly the one that makes use of single-fed digital antenna arrays. This is highlighted in the ZF beamforming use case, where even with SINR-based beam selection the LC-AAs perform better for SNR larger than 15 dB. Moreover, we notice that the curves of regularized ZFBF and standard ZFBF are identical in the high-SNR regime, as expected. Furthermore, Fig. 2a demonstrates that the use of CSI feedback instead of SINR feedback in the beam selection process improves substantially the performance. In the subsequent test scenarios, CSI-based beam selection is considered.

In Fig. 2b the sum-SE of regularized ZFBF for various IPT values as well as against its performance at the absence of a PS is depicted. We note that the throughput loss gets large, and the sum-SE eventually floors, for stringent IPTs.

In Fig. 2c the performance of ZFBF against its SL counterpart is compared. The use of binary phase shift key (BPSK) modulation is assumed and the IPT is $P_I = 15$ dB. We notice that SL-ZFBF outperforms significantly ZFBF in low SNR values but its capacity floors in the high-SNR regime since it does not completely eliminate the CCI.

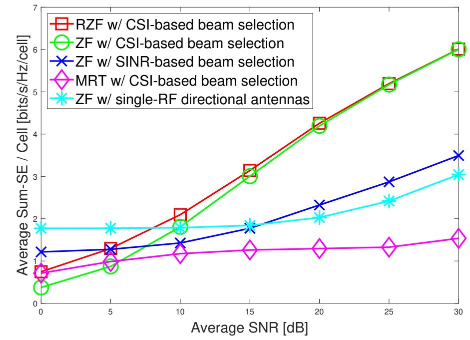

(a) Different beam selection and precoding variants for $P_I = 30$ dB.

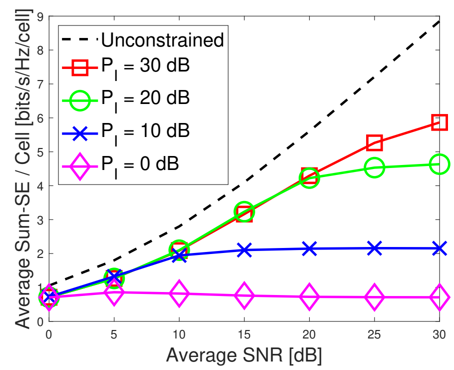

(b) Different IPTs.

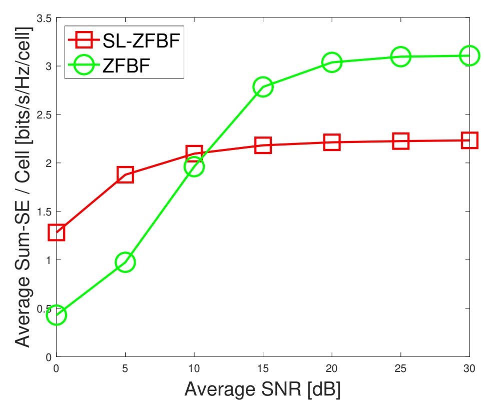

(c) SL-ZFBF vs. ZFBF for $P_I = 15$ dB.

Fig. 2: Average sum-SE / cell vs. average SNR for various scenarios.

9. SUMMARY AND CONCLUSIONS

A coordinated power allocation strategy that maximizes the sum-SE of cellular networks in NOSS setups under the application of well-known linear or SL precoding schemes is derived in this work. Numerical simulations indicate that this technique performs significantly well for small-to-moderate IPT values and highlight the performance gains of LC-AAs and SL precoding.

10. REFERENCES

[1] 3GPP, "TS 38.101-1 v.15.3.0 (2018/09)," technical specification, Sept. 2018.

[2] IEEE SIG Cognitive Radio in 5G, "Novel spectrum usage paradigms for 5G," white paper, Nov. 2014.

[3] 5G Americas, "5G services and use cases," white paper, Nov. 2017.

[4] N. Taramas et al., "Opportunistic beamforming for secondary users in licensed shared access networks," in *6th International Symposium on Communications, Control and Signal Processing (ISCCSP)*, Athens, Greece, 2014, 21-23 May.

[5] K. Ntougias et al., "Low-feedback cooperative opportunistic transmission for dynamic licensed shared access," in *European Signal Processing Conference (EUSIPCO)*, Nice, France, 2015, pp. 1222–1226, 31 Aug. - 4 Sept.

[6] S. Pandit and G. Singh, "An overview of spectrum sharing techniques in cognitive radio communication system," *Wireless Networks*, vol. 23, no. 2, pp. 497–518, Feb. 2017.

[7] E. Bjornson and E. Jorswieck, "Optimal resource allocation in coordinated multi-cell systems," *Foundations and Trends in Communications and Information Theory*, vol. 9, no. 2-3, pp. 113–381, Jan. 2013.

[8] D. Denkovski et al., "Generic multiuser coordinated beamforming for underlay spectrum sharing," *IEEE Transactions on Communications*, vol. 64, no. 6, pp. 2285–2298, June 2016.

[9] Antonis Kalis et al., Eds., *Parasitic antenna arrays for wireless MIMO systems*, In Kalis et al. [9], 2014.

[10] V. Barousis and C. B. Papadias, "Arbitrary precoding with single-fed parasitic arrays: Closed-form expressions and design guidelines," *IEEE Wireless Communications Letters*, vol. 3, no. 2, pp. 229–232, February 2014.

[11] G. Alexandropoulos et al., "Precoding for multiuser MIMO systems with single-fed parasitic antenna arrays," in *IEEE Global Communications Conference (GLOBECOM)*, Austin, TX, USA, December 8-12 2014, pp. 3897–3902.

[12] K. Ntougias, D. Ntaikos, and C. B. Papadias, "Coordinated MIMO with single-fed load-controlled parasitic antenna arrays," in *IEEE Signal Processing Advances in Wireless Communications (SPAWC)*, Edinburgh, UK, 2016, 3-6 July 2016.

[13] K. Ntougias, D. Ntaikos, and C. B. Papadias, "Robust low-complexity arbitrary user- and symbol-level multi-cell precoding with single-fed load-controlled parasitic antenna arrays," in *International Conference on Telecommunications (ICT)*, Thessaloniki, Greece, 2016, 16-18 May.

[14] K. Ntougias, D. Ntaikos, and C. B. Papadias, chapter Channel-dependent precoding for multiuser access with load-controlled parasitic antenna arrays, in *A. G. Kanatas, K. S. Nikita and P. Mathiopoulos (Eds.), New directions in wireless communications systems: From mobile to 5G*, CRC Press, 1st edition, pp. 279-314, Oct. 2017.

[15] K. Ntougias et al., "Large load-controlled multiple-active multiple-passive antenna arrays: Transmit beamforming and multi-user precoding," in *European Signal Processing Conference (EUSIPCO)*, Kos, Greece, 2017, 28 Aug.-2 Sept. 2017.

[16] P. Marsch and G. Fettweis, Eds., *Coordinated multipoint in mobile communications: From theory to practice*, Cambridge University Press, 2011.

[17] B. Clerckx and C. Oestges, *MIMO wireless networks*, Academic Press, second edition, Jan. 2013.

[18] E. Castaneda et al., "An overview on resource allocation techniques for multi-user MIMO systems," *IEEE Communications Surveys & Tutorials*, vol. 19, no. 1, pp. 239–284, 2017, First Quarter 2017.

[19] H. Huang et al., Eds., *MIMO communication for cellular networks*, Springer-Verlag New York, 2012.

[20] R. Zhang and Y. C. Liang, "Exploiting multi-antennas for opportunistic spectrum sharing in cognitive radio networks," *IEEE Journal of Selected Topics in Signal Processing*, vol. 2, no. 1, pp. 88–102, Feb. 2008.

[21] C. Masouros and E. Alsusa, "Dynamic linear precoding for the exploitation of known interference in MIMO broadcast systems," *IEEE Transactions on Wireless Communications*, vol. 8, no. 3, pp. 1396–1404, March 2009.